Complementarity between Quantum and Classical Mechanics in Chemical Modeling. The H + HeH^+ → H_2^+ + He Reaction: a Rigourous Test for Reaction Dynamics Methods.

Fabrizio Esposito,[*,†] Carla Maria Coppola,[‡,¶] and Dario De Fazio[*,§]

†*Istituto di Nanotecnologia - C.N.R., 70126, Bari, Italy*

‡ *Dipartimento di Chimica - Università degli Studi, 70126, Bari, Italy*

¶*INAF-Osservatorio Astrofisico di Arcetri, 50125, Firenze, Italy*

§*Istituto di Struttura della Materia - C.N.R., 00016, Roma, Italy*

E-mail: fabrizio.esposito@cnr.it; defazio.dario@yahoo.it

Abstract

In this work we present a dynamical study of the H + HeH^+ → H_2^+ + He reaction in a collision energy range from 0.1 meV to 10 eV, suitable to be used in applicative models. The paper extends and complements a recent work [*Phys. Chem. Chem. Phys.*, 2014, 16, 1162] devoted to the characterization of the reactivity from the ultra-cold regime up to the three-body dissociation breakup. In particular, the accuracy of the quasi-classical trajectory method below the three-body dissociation threshold has been assessed by a detailed comparison with previous calculations performed with different reaction dynamics methods, while the reliability of the results in the high energy range

has been checked by a direct comparison with the available experimental data. Integral cross sections for several HeH^+ roto-vibrational states have been analyzed and used to understand the extent of quantum effects in the reaction dynamics. By using quasi-classical trajectory method and quantum mechanical close coupling data, respectively in the high and low collision energy ranges, we obtain highly accurate thermal rate costants until 15,000 K including all (178) the roto-vibrational bound and quasi-bound states of HeH^+. The role of the collision induced dissociation is also discussed and explicitly calculated for the ground roto-vibrational state of HeH^+.

1 Introduction

The study of the reaction dynamics of elementary chemical processes in gas phase has great impact in many fields of scientific and technological interest, such as plasma[1,2] and combustion chemistry[3], aerothermodynamics[4–6], nuclear fusion[7], astrochemistry[8,9] and atmospheric kinetics[10]. These fields are investigated by setting up complex kinetic models, using as input detailed data of the main elementary processes intervening in the specific phenomenon of interest. Except for some specific collisional system (see e.g. Ref.[11]), the level of detail as well as the amount of data required[12] can hardly be found in literature when only experimental results are considered. Often some thermally averaged quantities are obtained experimentally, and then detailed data are extracted using some simplifying hypotheses and models[13]. On the other side, the direct calculation of detailed kinetic data, in the form of integral cross sections or rate coefficients for a large variety of processes and conditions, has been performed at different levels of approximation over the years. In particular, for most of the chemical networks, data as input of modeling are commonly obtained by using simplified assumptions[14,15]. In the past, simple approaches were justified by the lack of feasible molecular dynamics methods. However, thanks to the advance in the theoretical methodologies and computational technologies, it is now possible to obtain state resolved observables, with a large variety of dynamical methods with different degrees of approximation and computa-

tional costs. This allows to describe at least the simplest chemical networks by a complete state-to-state approach. When accurately calculated, detailed data can give important differences in the modeling[6,16]. In particular, the quasi-classical trajectory (QCT) method is commonly used for obtaining kinetic data[17], because of the good compromise between required accuracy and computational resources. On the other hand, quantum dynamical effects could play a relevant role for a realistic description of some applicative systems, in particular when low temperatures and low masses are involved.

Although a time independent quantum mechanical close coupling (QM-CC) approach is now affordable for a considerable number of chemical systems[18] also for calculating thermal rate constants in relatively large ranges of temperatures[19–23], it is clear that a complete quantum description also of the simplest chemical network is unfeasible, considering the large variety of processes often involved in applied chemistry and the large ranges of collisional energies usually required by models. As an example, relevant for the system here studied, we can report the difficulty to describe the motion of three free particles in time-independent quantum mechanical theory (see e.g. Ref.[24] and references therein) that allow to obtain QM-CC collision induced dissociation (CID) cross sections just for few prototypical systems in narrow ranges of collision energies[25]. The study of the CID dynamics by quantum wave packet methods[26] is easier than by QM-CC method, although at the state-of-the-art of the reaction dynamics quantum CID cross sections in a significant range of collision energies have been obtained only using drastic approximations to the reaction dynamics[27,28]. Easier and likely more reliable is the description of the CID dynamics in classical terms[29], considering that QCT calculations directly take into account the competition between the reaction and the dissociation channels[30,31].

The search for a computationally efficient methodology able to describe the complexity of a chemical system conserving the accuracy of QM-CC methods is a topic that has been studied since the early works on reaction dynamics[32,33]. One possibility is to introduce mathematical approximations in the kinetics[34–36] or in the state-to-state quantum reaction

dynamics[37–41] to reduce the computational effort. However the accuracy of these methods is often difficult to be known *a priori* so that the range of applicability of the quantum approximations cannot be guessed without a comparison in a large range of collision energies with benchmark results, typically available just for the simplest prototypical systems (see e.g. Ref.[42]). Other possibilities are offered by semiclassical methods[43–46] exploiting the relatively large masses of atoms and molecules that allow to introduce quantum effects *ad hoc* in a classical dynamical framework (for a complete review on the subject, see Ref.[47]). However, rigorous semiclassical solutions are often more difficult to be obtained than the quantum exact ones. For this reason, the modern trend is to use semiclassical mechanics to interpret quantum effects in reaction dynamics[48–50], rather than for predictive scope.

The approach followed in this paper consists in calculating reaction rate constants using both QCT and QM-CC methods. The idea is to use quantum mechanics when it is really needed, substituting it with computationally cheaper quasi-classical calculations when this can safely be done. In particular, we use QCT to continue QM-CC calculations at relatively high energy, retaining the same level of accuracy, by comparing the two methods in a sufficiently large common range of total energies. The advantages of QCT with respect to the other approximate methods consist in its simplicity, the huge amount of literature on the topic with both methodological improvements and case studies, and last but not least, the natural convergence of quantum mechanical results to the classical ones for increasing total energy. Moreover, differently from approximate quantum approaches[37,38], it permits to treat with the same level of accuracy the dynamics of either ground or excited reactant states, being this a considerable advantage when a state resolved chemical network is required to properly describe the physical environment. In fact, it is well known that classical and quantum mechanics should converge to the same results at large enough energies. However, rigorous comparison between QM-CC and QCT results calculated with the same potential energy surface (PES) in an extended range of collision energies and reactants states are rather uncommon, so that it is not clear how high the 'matching energy' of the two methods should

be. Moreover, while for reactions involving heavy atoms it is easier to guess the reliability of the QCT method also for low collisional energy, it is more difficult and uncertain for lighter atoms and ions, where the kinetics is often dominated by quantum effects (in particular, tunneling[51] and resonances[52]). The aim of this study is to assess the reliability of QCT calculations for specific light atoms collisions as the total energy is progressively decreased comparing with highly accurate QM-CC results. It is also important to assess the practical feasibility of QM-CC calculations and the amount of computational resources required, as the energy is increased.

To reach this goal we calculate new QCT cross sections for the reaction

$$H + HeH^+ \rightarrow H_2^+ + He \tag{1}$$

and compare the results with recent partly published QM-CC calculations[23]; moreover, additional comparisons are reported with other recent quantum mechanical calculations[53,54] performed with different methods on the same PES[55]. The chosen reaction has relevant applications; eventually, the calculated rate constants can be directly applied into models. Beside its relevance in the hydrogen plasma chemistry, process 1 is a fundamental pathway for the formation of molecular hydrogen cation in the early Universe[9,56–58]. Concerning these last models, however, in order to include correctly this process in the master equation, rate constants in a collision energy range of four orders of magnitude should be inserted, because of the rapid adiabatic expansion (and the consequent cooling) of the Universe in its first ages after the atomic recombination era. In this range of temperatures, of course, different processes (e.g. non-adiabatic[59] and collision induced dynamics) of the HeH_2^+ system can be relevant, so that a pure quantum mechanical approach, although extended to cover a large range of temperatures, has important limitations.

The present work is organized as follows: in Sec. 2 some details of the chemical system and of the employed reaction dynamical methods are given; in Sec. 3 the results are shown and reported in different subsections. In particular, in Sec. 3.1 a comparison of quantum

and classical cross sections is presented, including also previous dynamical calculations. In Sec. 3.2 different reactants conditions are analyzed to understand the effect of rotational and vibrational energies on the results. In Sec. 3.3 QM-CC and QCT reactive rate constants are shown in a large range of temperature (10-15,000 K). Classical collision induced dissociation rate from the fundamental state of the reactants is also shown to understand the relevance of this process in the description of the reaction dynamics. Finally in Sec. 4 our conclusions and further remarks are drawn.

2 Details of the Calculations

2.1 The chemical system

The HeH_2^+ is a prototypical reactive system, which has received extensive attention in literature (see e.g. Refs.[60–62] and references therein). This is mainly due to the low number of electrons involved and the light nuclear masses, allowing important simplifications in the PES calculations as well as in the reaction dynamics treatments. However, several studies concern the He + H_2^+ endothermic reaction, while the inverse exothermic process, target of this work, has a much more recent history. To the best of our knowledge, no dynamical calculation was published before the work of Bovino et al[53] in 2011. This is surprising, because it is the simplest example of ionic exothermic barrierless reactions, a class of processes very common in the interstellar medium, and it is of high relevance in different astrophysical environments (see e.g. Refs.[63,64]). In Ref.[53] quantum dynamical calculations were presented and employed in a cosmological evolution model[65] to explore the effect of the quantum dynamical rates of the reaction 1 on the molecular abundances of the most important species present in the early Universe scenario. Later, a close coupling quantum reactive study[23] was performed on the same PES[55], suggesting that important discrepancies with the previous calculation in the high energy range were likely due to dynamical approximations[37–39] used in[53]. The accuracy of the close coupling quantum results was also corroborated by the work

of Ref.[54] where a wave packet approach including Coriolis couplings was used[66]. Similar considerations can also be done regarding the published experimental work. The difficulty to obtain a well-collimated molecular beam of ions as well as the relative low stability of the hydrohelium cation make measurements of the reaction 1 very rare in literature, so that the only available experimental data[67,68] belong to an early epoch of the molecular beam technique; therefore, they are not well detailed. Moreover, the close coupling results of Ref.[23], performed on the same reliable PES used in this work, cast doubts about the calibration of these first measurements. About the quantum chemistry calculations, a large number of PESs are nowadays available for the reaction of Eq. 1 (for a recent review see Ref.[62]). Including the zero point energies, the reaction is exothermic for about 0.8 eV (803.4 meV in the PES here employed[55]). Two potential wells are found, both in collinear geometry[60]. The deepest, corresponding to a real bound triatomic complex, have a near product geometry (with the He atom at one end of the H_2^+ molecule) and its equilibrium configuration is about 338 meV below the H_2^+ product valley. The other one have an insertion geometry (with the He atom between the two hydrogen atoms) and it is unstable (~ 0.68 eV) with respect to the product, but it is 0.07 eV below the reactant's minimum. The dynamic of the reaction (1) is expected to be very sensitive to this potential feature. A considerable progress in reproducing experimental cross sections[61] has been obtained using the PES of Ref.[60], widely employed in reactive dynamical studies. A particular aspect of this PES was that an hyperspherical mapping was used to generate the grid of the ab-initio points, optimizing the accuracy of the reaction dynamics results. The PES was also refined in Ref.[55] where a more accurate diatomic potential was used[62]. In this work we will use one of the fitting PESs proposed in Ref.[60] (namely the M=6 fit to the MRCI ab-initio energies). Although this is not the fit with the lowest root mean square deviation, we prefer to use it to allow for an unambiguous comparison with the previous theoretical data calculated on this PES[23,53,54]. Moreover, the results reported in Ref.[62] show that for the He + H_2^+ reaction the ics are scarcely dependent on the degree of the polynomial used to perform the fit. However, we want to stress that

none of the PESs published contains the correct long range behavior, as suggested by the long range multipolar expansion[69]. This could affect some of the published results especially in the low energy range, where the dynamics is strongly driven by the long range tail of the potential[70,71].

2.2 The Quasi Classical Trajectory Method

The method of calculation for quasiclassical trajectories is well known and widely used, with large literature explaining the topic (see e.g. Refs[72,73]). The code used in this work has been written from scratch by one of us[74]. It has been modified over the years to include distributed and parallel capabilities (it is now a "hybrid" code, parallelized using both MPI and multithread technologies). The code has been largely tested against many theoretical and experimental results both for light[29] and heavy[75–77] collisional systems. The integrator employed to calculate the trajectories is the well known fourth-order Runge-Kutta, although other algorithms are implemented and can be selected in the software. The numerical performance as well as the accuracy of the code have been greatly improved introducing a variable time step Δt with a continuous check of trajectory accuracy. This check is performed at each trajectory step by re-integrating with Δt/2 , and comparing the final positions and velocities obtained in the two cases with a predetermined level of tolerance (in this work 10^{-9}Å for positions and 10^{-9}Å$/fs$ for velocities). If the test fails, the integration with the smaller time step is retained and compared with a new more accurate integration, obtained using Δt/4, and so on. This procedure, counterintuitively, leads to a much better overall performance[78], because very often the trajectory can be safely integrated with a large and cheap time step, that compensates for the extra effort required by the double integration. The net result of this simple technique is a large gain in computational time for a given accuracy of trajectories, typically as large as one order of magnitude[78], with the extra advantage that each trajectory is accurately checked, contrarily to what happens with a statistical evaluation of accuracy with a fixed time step. The initial conditions are set using a value of 15 Å as the

maximum distance of interaction R_{max}, obtained by checking the convergence of the cross sections with an increasing value of this parameter at some representative collision energy values. Energy levels, minimum and maximum vibrational elongations and vibrational periods related to each state have been calculated from the diatomic asymptotic form of the three particle potential by semiclassical WKB method, as in Ref.[79]. A comparison with quantum mechanical energy levels of HeH^+ is presented in the supplementary material[80]. Discrepancy among levels in the two sets is from 0.1 to 0.6 meV. The best agreement is obtained for high lying rovibrational states. Final analysis of trajectories is performed by iterative search of rovibrational action matching[79]. Impact parameter b is selected from a quadratic distribution in an interval of 0.1 Å, starting from zero, using a stratified sampling that is stopped if there is no reaction and final continuous rotational and vibrational pseudo-quantum numbers in the non-reactive case differ from their respective quantized values in the reactants by less than 0.2. Final analysis is performed by histogram binning technique. Concerning this last topic, it is worth noting that, although other binning strategies have been proposed[47,81], exothermic barrierless reactions are generally not affected by binning and zero point energy issues[47,82]. This is not valid for the reverse He + H_2^+ reaction where zero point energy corrections significantly affect the QCT ics values[30]. From 10,000 to 56,000 trajectories have been run for each collisional energy of each HeH^+ roto-vibrational state, in total not less than 650 millions of trajectories have been calculated.

2.3 Quantum reactive scattering calculations

Time independent quantum reactive scattering calculations are essentially the same published in Ref.[23] and the details of the implementation and the used input parameters can be found therein (see Table 1 of Ref.[23]). Just a brief summary will be given here. The quantum mechanical calculations have been performed using a modified and parallelized version[83] of the ABC code of Manolopoulos and co-workers[84]. The most important modification is the implementation of an Enhanced Renormalized Numerov method[85], replacing

the log derivative propagator[86] implemented in the original code, to propagate the hyperradial wavefunctions. This makes the calculation more efficient (from one order of magnitude down to a factor two) especially in the low collision energy range[23]. A large number (16) of projections of the Total Angular Momentum into the body fixed frame has been used to obtain convergent numerical data within few tenths of percent. The calculation exploits the symmetry of the PES with respect to exchange of the two hydrogen atoms, by applying the principle of microscopic reversibility directly on the S-matrix elements calculated for the reverse (He + H_2^+) reaction. Integral cross sections have been also appropriately post-antisymmetrized[87] to take into account the effect of the nuclear spin statistics. However, as shown in Ref.[23], the effects of the anti-symmetrization are very small for total integral cross section (hereafter referred to as ics) and completely negligible for rate constants; therefore, the comparison with QCT results, not using post-antisymmetrization procedure, can safely be done.

3 Results and Discussion

3.1 Integral Cross Sections

In Fig. 1 QCT and QM-CC total ics of reaction 1 with the molecular ion in its ground state are shown on a logarithmic scale. A large center of mass kinetic energy range is reported (from 0.1 meV to 10 eV). The comparison between the two methods is possible only below 1.25 eV because of the mathematical difficulties, reported in Sec. 1, to describe the CID by QM-CC methods.

In the range of energy where the two calculations overlap, three regions are clearly distinguishable. Starting from the right of the figure, the first one is from 1.25 eV down to 0.15 eV, where the two ics are almost superimposed. The second region is located between 0.15 eV down to 40 meV. Here the agreement is fairly good on the average, with a slight systematic underestimation of the reactivity by the QCT results, probably due to the pres-

ence of resonance features. These features are much more pronounced in the third energy range, from 40 meV downward, where the classical results, clearly lower than QM-CC ics, rapidly decrease to zero, becoming negligible at a collision energy of about 1 meV. On the contrary, the QM-CC ics decreases towards a constant value, justified by the exothermicity of the reaction (for energies lower than those in Fig.1 the ics raises again to reach the Wigner threshold law behaviour[23]). The trend for energies higher than 1.25 eV, available only for QCT calculations, appears also reasonable, as it will be shown later by a comparison with the available experimental data[68].

In the inset of Fig. 1, an approximate comparison between the computational load as a function of the collision energy is reported. In the QCT case, the load is obtained as the computational time per trajectory, normalized to the highest value. A rapid decrease with the increase of the collision energy is shown, with a final value two orders of magnitude lower than the initial one. This is expected because the trajectory integrator takes more steps to complete a slower trajectory, although an optimized variable time step is used. The normalized computational load of QM-CC calculations is evaluated considering the convergent number of total angular momentum and of its projections used (see Table 1 of Ref.[23]), normalized with the value obtained in the highest energy range. Also in this case the ratio between the maximum and the minimum values of the normalized computational load is about two orders of magnitude, but the trends are completely inverted with respect to the QCT calculation. Of course, the curves plotted in the inset of Fig. 1 give information just on the behaviour of the computational cost as a function of the collision energy of the two different methodologies; however, they do not allow for a direct absolute comparison between them. In fact, several considerations make a rigourous comparison very hard to be achieved and specific for the particular output considered. For example, in the QM-CC case, several collision energies in a particular energy range are calculated simultaneously, with small computational differences if the energy discretization is fine or rough. On the other hand the computational cost for QCT scales linearly with the number of energies

calculated. In addition, in the QM-CC calculation the full S-matrix is obtained, therefore a single calculation allows in principle to obtain all the ro-vibrational transitions open at a specific total energy. This is not the case for QCT, where a new calculation must be done for each reactant state considered. However, considering just the normalized quantities, each referred to its own computational method with its peculiarities, it is interesting and impressive to see the specular trends of the computational costs for the two calculations. These intersecting trends are both in the same most convenient direction with respect to the obtained results. In fact, where the exact QM method is (relatively) very cheap, at low energy, it is also needed, because the classical result is very unreliable and (relatively) very expensive, while the QCT method is very cheap and accurate at high energy values, where QM-CC is very expensive.

In Fig. 1 QM-CC and QCT cross sections are also compared with other results obtained by different quantum dynamical methods on the same PES[55]. In particular we report the recent result by Gamallo et al.[54], calculated by a wave packet (WP) method[66] including Coriolis coupling, together with the approximate quantum mechanical result of Ref.[53], using centrifugal sudden (CS) and reactive infinite order sudden (RIOSA) approximations[37,38] together with a negative imaginary absorbing potential (NIP)[39]. The quantum methods are essentially in good agreement in the low collision energy range from 0.1 meV up to 20 meV (larger differences are detected in the cold and ultra-cold regimes[23,54]). At higher collision energies there is a clear drop of the QM-CS/NIP ics, with 40% discrepancy somewhere with respect to the other QM methods and a relevant underestimation of the reactivity that is maintained also for energies close to 1 eV. This is probably due to the high relevance of the Coriolis coupling for this reaction, neglected by the CS approximation[23,54]. The QM-WP result, using the same number of projections of the total angular momentum, appears very similar to the QM-CC one on the whole energy range, with discrepancies smaller than 10%. However, for collision energies greater than 70 meV, the agreement with QM-CC results is much better for QCT than for QM-WP, notwithstanding this calculation is claimed to be

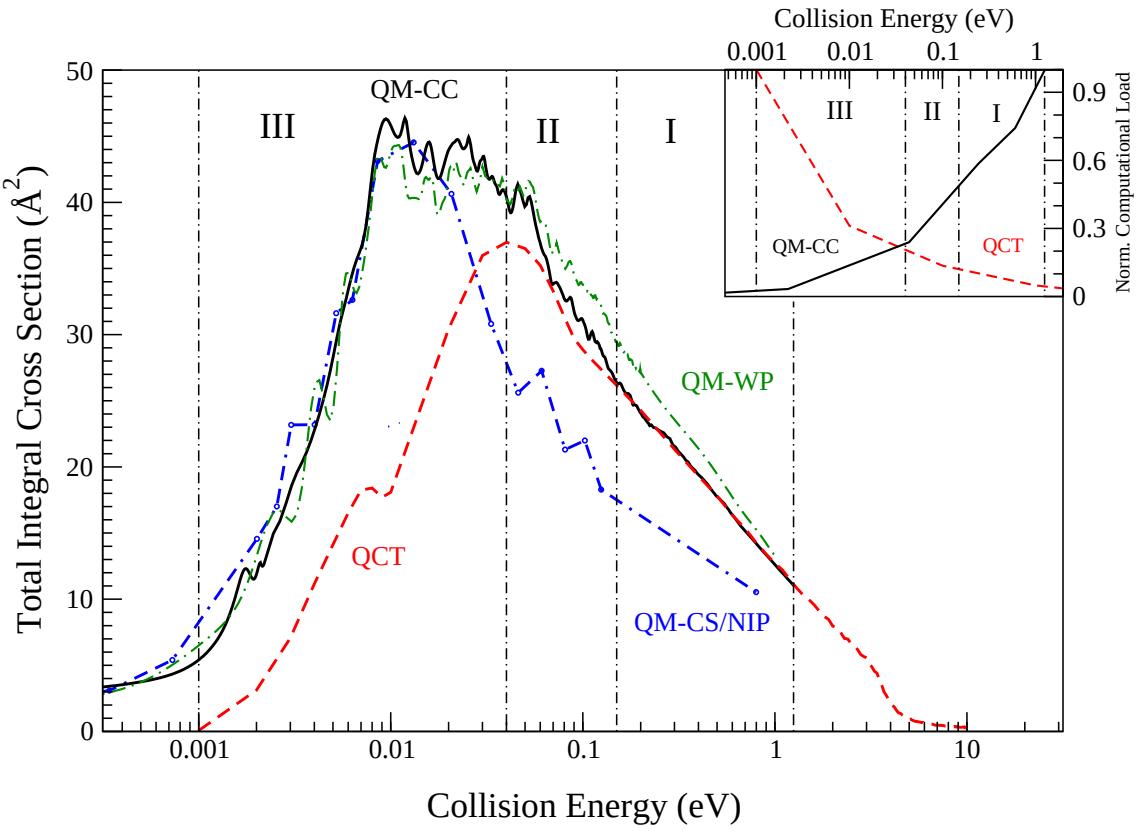

Figure 1 Esposito et al

Figure 1: Comparison among total integral cross sections for the H + $HeH^+(v{=}0,j{=}0) \rightarrow He + H_2^+$ reaction obtained with different dynamical methods. All the theoretical results have been obtained using the RMRCI6 PES[55]. Solid black and red dashed lines are QM-CC and QCT results. Green dot dashed and blue dot dashed dashed lines are QM-WP and QM-CS/NIP results published by Gamallo et al.[54] and Bovino et al.[53] respectively. Black dot dashed lines define three different regimes of comparison (see text for details). In the inset, a comparison between QCT and QM-CC normalized computational load estimations is given (see text for definitions).

accurate within 2%. It is worth focusing on this level of agreement of QCT results with respect to the most accurate ones; indeed, very often QCT are considered less reliable than QM calculations, unless a very high collisional energy range (typically higher than 10 eV) is studied. On the contrary, studying carefully the correct range of applicability, the use of classical mechanics can be computationally very convenient and numerically accurate also in the intermediate energy range, at least for the class of chemical processes to which reaction 1 belongs.

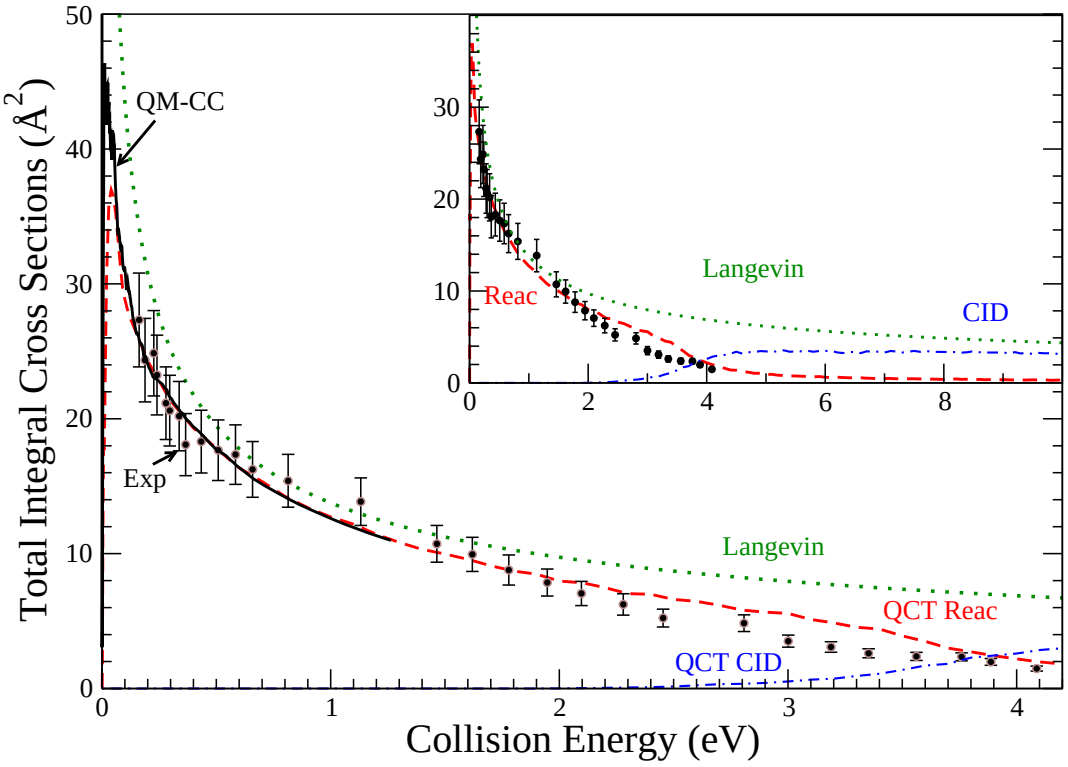

Figure 2 Esposito et al

Figure 2: Comparison between total ics for the H + $HeH^+(v{=}0,j{=}0)$ reactants and the experimental results of Ref.[68] (filled circles with error bars). Black solid and red dashed lines are as in Fig. 1. Blue dot dashed line are the QCT total ics for the CID channel. Also reported as dotted green line are the ics predicted by Langevin model[23,88]. The absolute experimental value of Ref.[68] are rescaled as in Ref.[23] to match with QM-CC result and represented by black filled circles. The inset shows the same comparison in a more extended collision energy range.

In Fig. 2 the integral cross sections for reaction 1 calculated using different methods and involving HeH^+ in the ground roto-vibrational state are plotted on a linear scale, in order to compare with the experimental data of Ref.[68]. The original absolute experimental values are scaled by a costant factor of 2.358 to optimize the comparison with QM-CC theoretical data[23]. As shown in the figure, the good agreement between theoretical and scaled experimental data is confirmed also in the high collision energy region, supporting the hypothesis of an inaccurate calibration of the experimental data, possibly due to an unreliable estimation of the degree of dissociation of the hydrogen molecules heated in the furnace[68]. Actually, considering the error bars of the experiments, the comparison in the high energy range is slightly worse around 3 eV; in particular, the experimental result is slightly higher than the theoretical ics up to 2.0 eV and lower for higher energies. In the following section we will give some suggestions about the possible origin of these minor discrepancies. In the same figure also QCT-CID and the results obtained by the Langevin model[88] are reported. We note that although the CID channel opens at around 1.85 eV, it represents an almost negligible pathway until $\sim$ 3 eV, where gradually it starts to increase reaching the reactive ics value around 4 eV. Dissociation dynamical threshold is very near to energy threshold (discrepancy is less than 0.05eV), and this is a good indication that the classical calculation for dissociation is reliable for this kind of collision[89–91]. The simple Langevin model describes the reactivity reasonably well (within about 20%) in the range 0.5-2 eV. However at higher collision energy the agreement becomes gradually worse. This can be rationalized taking into account the following considerations. In the inset of Fig. 2 we show the comparison in the full range of collision energy (0.1-10 eV). The inset suggests that the agreement with the model is still good in the high collision energy range, if the sum between the CID and the reactive pathways is considered. This is reasonable, considering that the simple Langevin result is based on a capture model that cannot take into account the exact final product once the strong coupling region is reached.

3.2 Roto-vibrational Effects

In Fig. 3 QM-CC and QCT ics are compared for different rotational states of the reactants, from j=0 to j=5. The figure clearly shows very good agreement between QCT and QM-CC results for HeH^+ excited rotational states; in particular, from j = 2 onward the 'matching energy' between QM-CC and QCT drops down to 6 meV. It is worth noting the increasing agreement between QM-CC and QCT for high rotational states. However, we can note

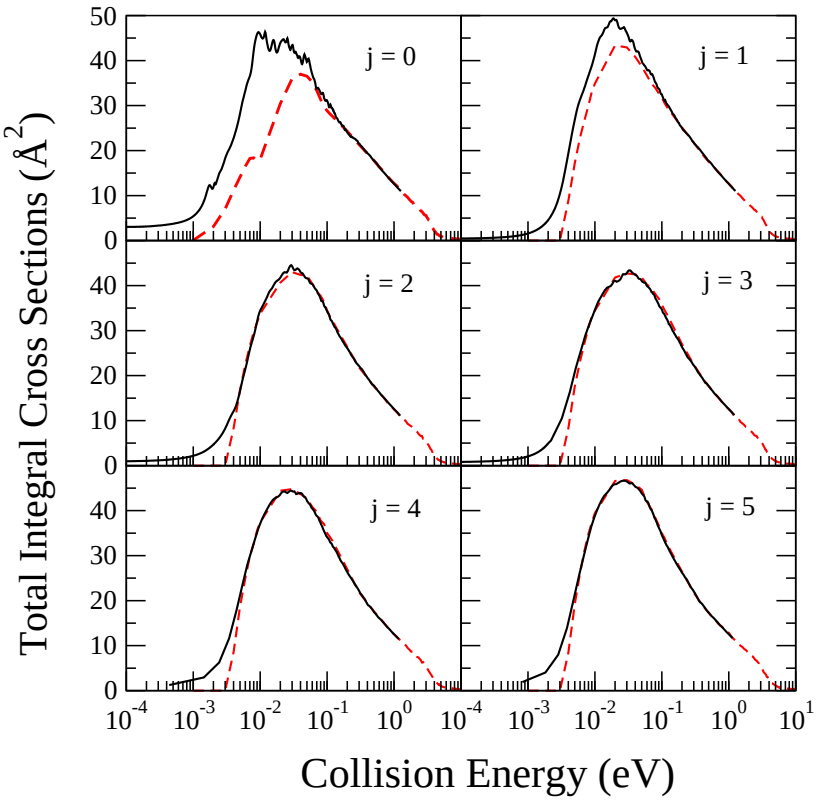

Figure 3 Esposito et al

Figure 3: Comparison between total ics for excited reactant rotational states from 0 to 5. Black solid and red dashed lines are as in Fig. 1. The reactant rotational state is as indicated inside each panel.

that the first two rotational states are the only ones showing oscillations in the QM-CC ics; this feature is not reproduced in the quasiclassical results. Thus, this discrepancy could be due to purely quantum mechanical effects as resonance phenomena[52] (that could be

analyzed, for example, using the complex angular momentum theory[92]), or a tunneling effect through a tiny long range reactive barrier. This last hypothesis is reasonable considering that the root mean square of the PES fitting is comparable to the rotational constant of HeH^+ and that its strong dipole moment can facilitate the energy transfer between the rotational and translational degrees of freedom. From a practical point of view, the results of Fig. 3 suggest that for modeling applications QM calculations are necessary to correct the low energy behaviour of the reactants lowest rotational states, while QCT results can be safely used to obtain a realistic description for the reactivity of excited rotational states. We note that the good agreement between QCT and QM-CC results for excited reactants rotational states is in contrast with the results in Ref.[93] where the quantum approximation used appears inadequate for the accurate description of excited state (see discussions in Ref.[23]). A comparison among the curves in Fig. 3 shows that rotational effects are completely negligible above 250 meV and very small also at low collision energies. More relevant are the effects of the reactant vibrational energy on the reactivity.

In Fig. 4 QCT ics for the ground rotational level of the even vibrational states are reported, together with their statistical error bars, from v=0 to $v = 4$. Odd states (not shown) show similar intermediate behaviours. On the same figure we also report the experimental values, with their error bars. We note that adding two vibrational quanta of the reactant energy, the ics values are higher than the v=0 ics for collision energy in the range 0.4-2.5 eV and lower for higher energies. The inversion point for this vibrational effect decreases as additional quanta are added, reaching about 1.7 eV for v=4. We note that these vibrational effects are in the direction of discrepancies with the experimental results described in the previous section, suggesting a possible contamination of excited vibrational states in the molecular beam used in Ref.[68]. This hypothesis is reasonable considering also the epoch in which this experiment has been carried out and that no comments with respect to the state selected beam purity is reported in that paper. The lower reactivity of higher vibrational states at high collision energy, and its sistematic behaviour with v, can be easily understood

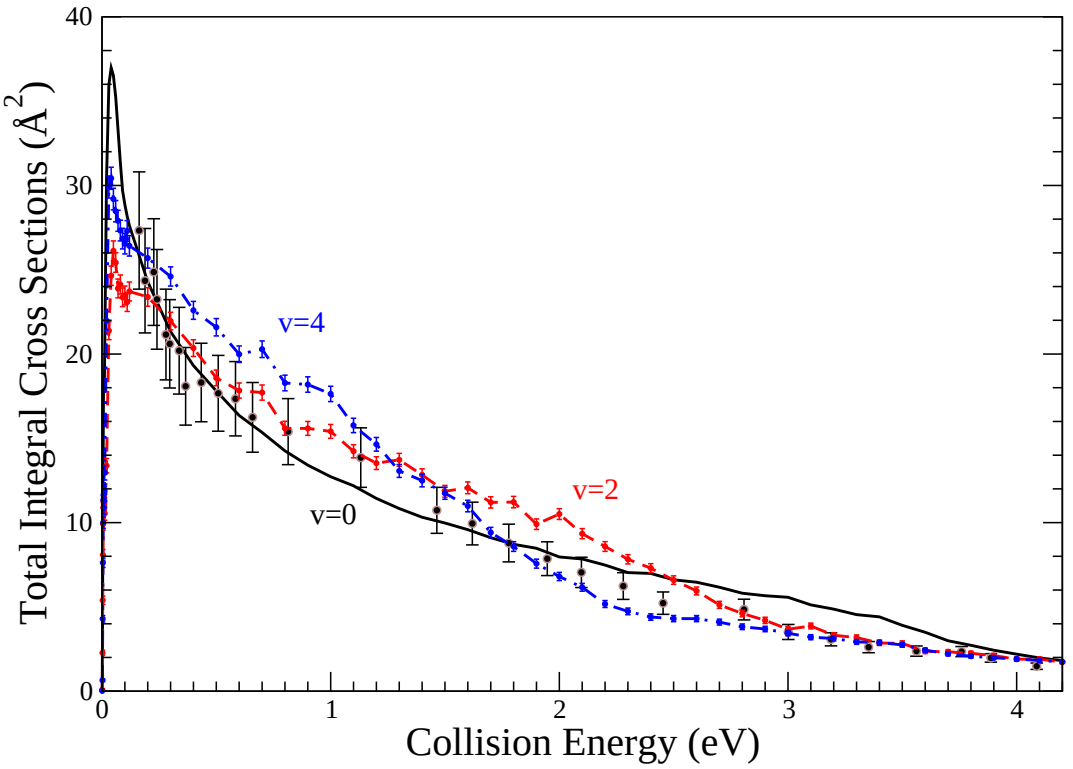

Figure 4 Esposito et al

Figure 4: QCT total ics for j=0 of even excited reactant vibrational states from 0 to 4. Black solid, red dashed and blue dot dashed lines are for v=0, 2 and 4 respectively. Also reported are QCT statistical error bars of the excited reactants states. Experimental data with error bars are shown with black filled circles, as in Fig. 2.

considering that the CID collision energy threshold becomes sistematically lower at high v (this can be appreciated by inspecting the table provided in the supplementary material), so that the competition with the CID pathway becomes more relevant. Finally, we can also note that the QCT integral cross sections of higher v states exhibit some oscillations not present in the ics of the reactants ground vibrational state. At these relatively high total energies, in the neighborhood of the CID threshold, QM-CC calculations can not be done, so that the existence of these features can not be checked by a direct comparison. In general, however, with the increase of the total energy the conditions become more classical, so an increasing accuracy of QCT trajectories is expected.

3.3 Rate coefficients

Initial state selected rate coefficients can be obtained by translationally averaging the state-to-state cross sections, $\sigma_{v,j;v',j'}(E)$ summed over the product quantum numbers v' and j':

$$k_{v,j}(T) = \sqrt{\frac{8}{\mu\pi(k_B T)^3}} \cdot \int E \sum_{v',j'} \sigma_{v,j;v',j'}(E) \exp(-E/(k_B T)) dE \tag{2}$$

where μ is the reduced mass of the H+HeH$^+$ system, k_B is the Boltzmann constant and T is the translational temperature.

In Fig. 5 a comparison among rate coefficients obtained for reactants in $(v = 0, j = 0)$ state is shown. Such quantities are largely used in applicative models and this approach is usually referred to as *ground state approximation*. It consists in considering the reactivity as independent of the reactant roto-vibrational quantum numbers. As a consequence, the rate constant can be directly calculated by integrating the total ics of the ground state reaction. In Ref.[23] it has been shown that for this specific reaction the ground state approximation works very well, at least until 2,000 K, within an accuracy of about 7%. Clearly, this is a consequence of the small relevance on the reactivity of the reactant rotational and vibrational

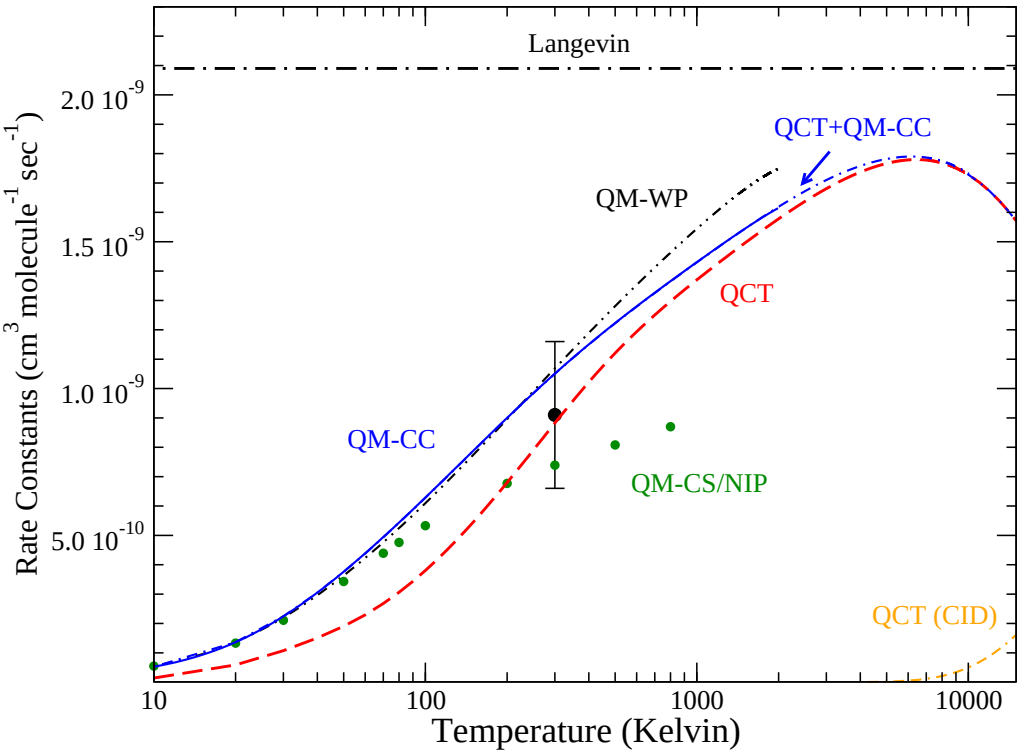

Figure 5 Esposito et al

Figure 5: Comparison among rate constants in ground state approximation obtained with different dynamical methods. All the theoretical results have been obtained using the RM-RCI6 PES[55]. Solid blue, red dashed, brown dot dot dashed lines and filled green circles are for QM-CC[23], QCT (present result), QM-WP[54] and QM-CS/NIP[53] results respectively. Blue dot dashed line is our best estimation obtained integrating a mixed QM-CC/QCT ($v = 0, j = 0$) ics (see text for details). Also reported as an orange dashed dashed dot and as black dot dashed lines are the rate obtained integrating CID ics and the results of the Langevin model[88] respectively. Black full circle with error bar is the experimental measurement of Ref.[67].

effects discussed in the previous section. In the same figure the Langevin costant value of 2.088×10^{-9} cm^{-3} sec^{-1} and the experimental result by Karpas et al.[67] are also reported. From the comparison among the curves we can note that below 70 K all the QM results are almost coincident. In this range of temperature, QCT results are about one half of the QM rates. However, around 100 K QM approximate ics increases with a lower slope than the other results, so that at around 200 K the reaction rate is smaller than the results obtained with the other QM methods. At higher temperatures, QCT reaction rate increases faster than QM-CC so that at room temperature (close to the experimental temperature) the difference with QM-CC is less than 15%. Until this temperature, QM-WP rate agrees within the numerical accuracy of the data (1-2%) with QM-CC. We note that all the methods are able to reproduce the experimental value, within its large error bar; incidentally, the QCT rate shows the closest agreement. In the range 300-2,000 K QM-WP rate gradually starts to become higher than the QM-CC results, so that at 2,000 K the deviation between QM-WP and QM-CC rate coefficients is larger than the deviation between QCT and QM-CC results (differently from the room temperature case). The difference between QM-WP and QM-CC results is due to the slight ics discrepancies seen in Fig. 1; it could appear surprising considering that both methods can be considered essentially 'exact' methodologies and that the claimed accuracy of theoretical data is lower than the found discrepancy (slightly higher than 10%). However, in Ref.[54] only some of the partial waves have been actually calculated and an interpolation procedure has been adopted for all the others, in order to save computational time. The procedure was claimed to reproduce ics within an accuracy of about 2-3%[54] but it is possible that at high energies, where a large number of partial waves is required, the real accuracy of the data becomes lower. Another possibility is that the wave packet parameters used in Ref.[54] were not appropriate for high collision energies calculations[94]. QCT results continue to increase until about 6,000 K, where the rate shows a broad maximum ($\sim 1.8\ 10^{-9}$ cm^{-3} sec^{-1}), that is 10-15% below the Langevin constant value. As shown in the figure, this is also the temperature where the dissociation rate constant starts to be significant, indicating

that the feature is likely due to the competition between the reactive and CID channels. In the same figure a dot-dashed blue line is also shown, representing our best estimation of the rate and calculated integrating a mixed QM-CC/QCT ics. This optimal ics has been obtained using the QM-CC ics until $\sim$ 1.25 eV and QCT ics up to 10 eV. Given the level of agreement of the two integral cross sections around 1 eV, as shown in Fig. 1, the merging is completely smooth.

Thermal rate constants, averaged over the Boltzmann distributions of the rotovibrational states of HeH^+ can be written as:

$$k(T) = \frac{\sum_{v,j}(2j+1)\exp(-E_{v,j}/k_BT)k_{v,j}(T)}{\sum_{v,j}(2j+1)\exp(-E_{v,j}/k_BT)} \tag{3}$$

They are plotted in Fig. 6. To obtain QCT thermal rates all the 178 bound and quasi-bound roto-vibrational states (v_{max}=10, j_{max}=26) of the hydro-helium cation were included in the thermal averaging. The QM-CC thermal rate by Ref.[23] is also shown. The solid black curve is obtained using QM-CC/QCT mixed integral cross sections for $v = 0$ and $j = 0 \rightarrow 5$ in Eq. 2 and the QCT results for all the other HeH^+ roto-vibrational states, and finally averaging according to Eq. 3. It is evident that QM-CC/QCT curve smoothly merges the behaviours of the QM-CC and QCT results. We note that this behaviour of the kinetic data can not be described by the analytical fitting model functions, as the ones used in Refs.[23,51,95], often used to compact kinetic information in the master equations of chemical networks. This is because the competition with the CID channel, not included in most of the kinetic analytical models typically employed, as will be discussed later, markedly shapes the maximum feature. We therefore provide here a polynomial numerical fit for the total thermal reaction rate. The analytical function employed is:

$$k(T) = \sum_{i=0}^{7} a_i(\log_{10}T)^{\mathrm{i}} \tag{4}$$

and the obtained parameters (units: $cm^3\ s^{-1}$) are a_0=-4.45164$\times10^{-9}$, a_1=1.49207$\times10^{-8}$,

a_2=-1.97946×10^{-8}, a_3=1.32296×10^{-8}, a_4=-4.60313×10^{-9}, a_5=8.08319×10^{-10}, a_6=-5.67934×10^{-11}. The maximum error is less than 2.5%. Also reported in the figure is the reaction rate in

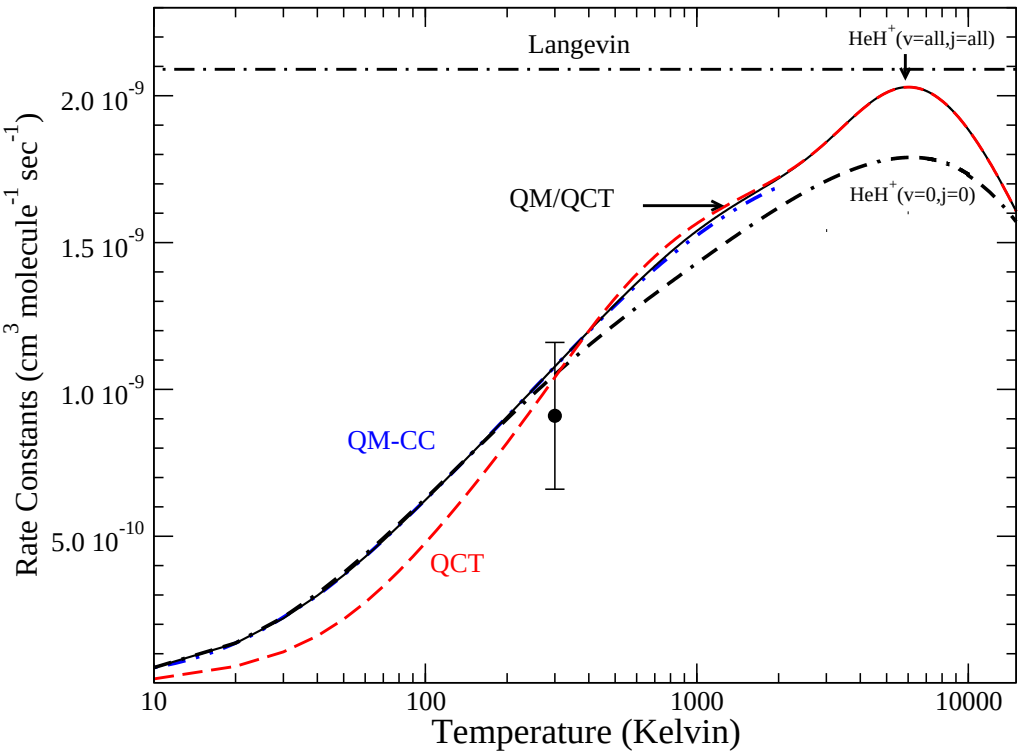

Figure 6 Esposito et al

Figure 6: Comparison among rate constants in ground state approximation with thermally averaged quantities. Dot-dot-dash blue and dash red lines are full convergent thermal averaged rates calculated with QM-CC[23] and QCT methods respectively. The solid black line are thermal rates using a mixed QM-CC/QCT database including all the reactants rovibrational states while the dashed-dashed-dot black line is the result obtained integrating only the ground state ics. Also reported as a black dot-dash line is the result of the Langevin model and the experimental measurement of Ref.[67] (black full circle with error bar).

the ground state approximation. The figure shows that this approximation is excellent until room temperature and that QCT results significantly underestimate the reactivity below 300 K, although the agreement with QM-CC curve is slightly better than in Fig. 5. This is actually due to the selective underestimation in QCT ics of the lowest reactant rotational

states reactivity, as shown in Fig. 3. Increasing the temperature the population of these states becomes lower and the difference between QCT and QM-CC thermal rates decreases significantly, so that at the temperature of the experiment the discrepancy is near to the sum of the numerical accuracies of the data ($\sim$2%). This is not surprising considering that at this temperature only 15% of HeH^+ is in its ground roto-vibrational state. In the range 300-2,000 K QM-CC and QCT thermal rates (solid lines) agree very well (within 3-4%). At higher temperatures, a large maximum just few percent below the Langevin value is shown (T $\sim$6000 K). We can note that the maximum is narrower with respect to the curve for the ground state approximation rate. It moves at lower T so that the ground state approximation becomes worse at high temperatures, giving rates with accuracy within about 20%. This effect is due to the lower energy threshold for the CID channel for higher vibrational states that make the CID pathway competitive with the reaction at lower temperatures. However, several issues limit the reliability of the results presented in this range of T. First, the validity of the Born-Oppenheimer approximation is largely questionable at total energy above $\sim$ 8 eV[96], where the reactive charge transfer pathway (leading to hydrogen molecule plus He^+) becomes open. These collision energies of course could affect the rates in the range 10,000-15,000 K so that kinetic effects of the competition of the non-adiabatic channels could significantly change the values of the rates. Nevertheless, preliminary studies of the excited electronic surfaces of the system[96] give indication that conical intersections involving charge transfer are located at very high total energies ($\sim$7.3 eV above the CID threshold for the ground state) so that just the ics tails are expected to be affected. Moreover, the expected presence of partial thermal dissociation in the highest range of T makes questionable[97] the thermal assumption used to calculate the rates. In fact, it is well known that, in presence of thermal dissociation, non-equilibrium effects arise in the roto-vibrational distribution, significantly affecting the reaction rate[98–101]. However, a more accurate kinetic calculation taking into account non-adiabatic and non-equilibrium effects is beyond the scope of the present publication.

4 Conclusions and Perspectives

The high complexity of most of the chemical networks involved in applied chemistry often does not allow to use a single methodology for calculating the large amount of kinetic data for the different processes typically needed. It is therefore crucial to know exactly the range of applicability of different dynamical methods to obtain accurate data to be used in the numerical simulations. In this work, this issue is investigated taking as an example the case study of the H + HeH^+ reaction, recently studied with different quantum mechanical methods[23,53,54] using the same electronic adiabatic potential energy surface[55]. To achieve this aim, a complete quasi-classical trajectory study of the dynamics from 0.1 meV to 10 eV in Born-Oppenheimer approximation has been performed and compared with the previous theoretical data and with available experimental measurements[67,68]. An excellent agreement with QM-CC and QCT results from 0.1 eV up to 1.25 eV is found (Fig. 1). The good agreement (Fig. 2) with the molecular beam data by Rutherford and Vroom[68] when the numerical factor suggested in Ref.[23] is applied to rescale the experiments, also supports the reliability of the QCT calculations up to the three-body breakup threshold. A complete study of the effect on the reactivity of the internal (roto-vibrational) energy of the reactants is also supplied (see Sec. 3.2). The rotational energy has small (almost negligible) effect on the integral cross sections that are perfectly reproduced by the QCT calculations for higher rotational states (Fig. 3). The vibrational energy affects more the reactive attributes (Fig. 4) and it could be responsible for the remaining small discrepancies with the scaled experimental data[68] in the high collision energy range (3-4 eV). The comparison with the other previous theoretical data[53,54] shows that QCT, differently from the other quantum methods, cannot properly describe the low energy behaviour of the ground state reaction rate (Fig. 1). However, starting from $\sim$0.1 eV, the QCT method has the closest agreement with the close coupling quantum data; this level of agreement is significantly better than the one of the approximate quantum method used in Ref.[53] and better than the wave packet calculation of Ref.[54], that solves the time dependent quantum mechanical problem without using any strong approximations.

This impressive result suggests an unusual hierarchy in the commonly believed reliability of approximated scattering methods at intermediate collision energies and it is likely general enough, at least for the class of exothermic ion-molecule barrierless reactions, for which reaction 1 is considered to be a prototype. The large computational efficiency of quantum and classical data, respectively in the low and high collision energy range (see Fig. 1), and the high level of agreement in the intermediate energy range under the CID threshold, suggest a highly accurate and efficient way to get detailed kinetic data to be used in applicative models. Classical and quantum data in the high and low collision energy ranges, respectively, are used together to obtain high reliable kinetic rate constants in a huge range of temperatures (until 15,000 K, see Fig. 6). Vibrational effects and especially the competition between reactive and dissociation pathways deeply influence the shape of the temperature dependence of the rate constants especially around 8,000 K, where is shown a clear maximum in the reactive yields, just below the capture theory Langevin value.

The common energy range is fundamental for clearly assessing the accuracy of QCT calculations. Interesting is the possibility to introduce at least a vibrational resolution of the chemical network, with expected strong effects on the chemical abundances of the main molecular species of the early Universe scenario. With this aim, a vibrational resolved analysis of the work done is presented in Appendix. More numerical studies by our group in this direction are still in progress.

Acknowledgement

We acknowledge the Italian MIUR for financial support by PRIN 2010/2011 grant N. 2010ERFKXL. The computational time was supplied by CINECA (Bologna) under ISCRA projects N. HP10CJX3D4 and HP10C7RZR8. Part of the scattering calculations was performed under the HPC-EUROPA2 programme (project number: HP10CIF3IN) with support of the European Commission - Capacities Area- Research. DDF and CMC acknowledges the

discussions within the international team #272 lead by C. M. Coppola "EUROPA - Early Universe: Research on Plasma Astrochemistry" at ISSI (International Space Science Institute) in Bern. The authors also thank Prof. Vincenzo Aquilanti (University of Perugia) and Prof. Savino Longo (University of Bari) for scientific discussions.

Supporting Information Available

Comparison between the energy levels of HeH^+ calculated using WKB (including the quasi-bound states) and QM methods. The former have been used in QCT calculations. The dissociation limit is considered as the zero, and the energies are given in eV. This material is available free of charge via the Internet at `http://pubs.acs.org/`.

A The vibrational resolved dynamics.

More information about the microscopic reaction mechanisms can be obtained by the analysis of the product vibrational distributions[102]. In Fig. 7 a comparison between some QM-CC and QCT integral cross sections for vibrationally resolved product of the roto-vibrational reactant's ground state reaction is shown. We can observe a significant agreement in the energy range indicated as region I in Fig. 1, although in some cases the convergence is at some higher collision energy (see for example $v' = 1$ in lower panel). At lower energies the integral cross sections show a relevant discrepancy, though with the same trend (see e.g. v'=2 curve of the upper panel of Fig. 7); this effect is more likely to be caused by a larger relevance in this energy range of the resonance patterns in the state-to-state ics (cf. Fig. 7 with Fig. 1), rather than to the binning strategy employed (histogram binning). The correct behaviour of QCT product vibrational distributions is relevant, for example, for cosmological applications, where reliable output of chemical evolution models in the early Universe requires a vibrational resolution of the chemical network, as recently suggested[8,101]. In such a state-to-state resolved approach to the chemical kinetics, the availability of a table

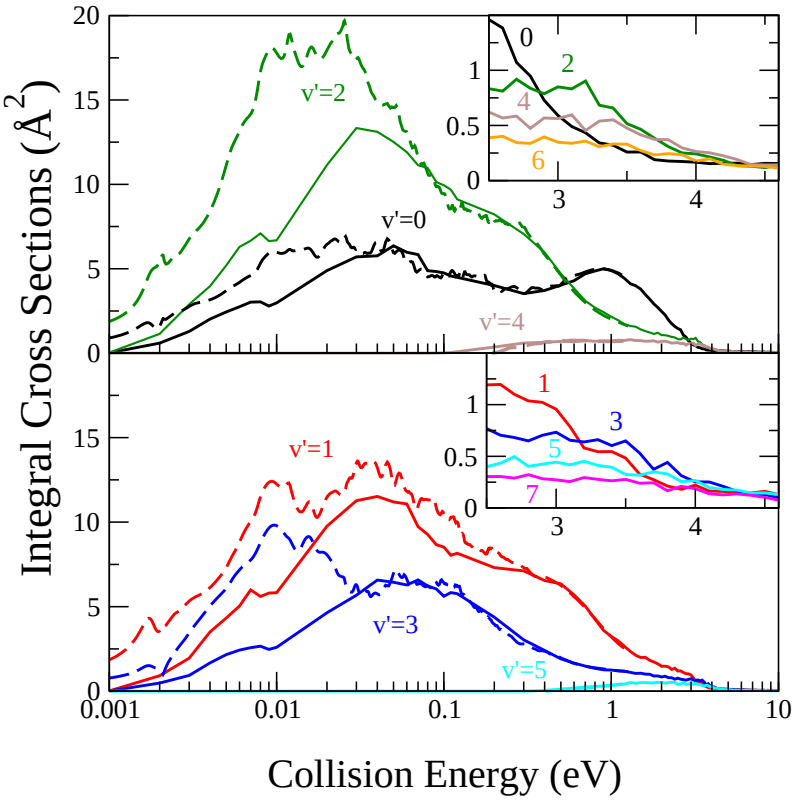

Figure 7 Esposito et al

Figure 7: Comparison between product vibrational ics for even (higher panel) and odd (lower panel) states and reactant's roto-vibrational ground level for reaction 1. Solid lines are QM-CC results while dashed line are QCT. The insets inside the panels show the ics behaviours at collision energies larger than 2.5 eV on a linear scale. Black, green, brown and orange colours are for v'=0,2,4 and 6 respectively (upper panel); red, blue, cyan and magenta colours are for v'=1,3,5 and 7 respectively (lower panel).

providing the complete reaction rate data set for all rotovibrational initial and final states is greatly useful and beneficial, rather than providing analytical fits.

It is worth noting that the product vibrational distributions show opposite behaviour at low and at high collision energies. In fact, at low collision energies (less than 100 meV) H_2^+ in higher vibrational levels is produced with a maximum for $v' = 2$. Otherwise, at collision energies higher than $\sim$ 1 eV, H_2^+ is mainly produced in its ground vibrational state (see Fig. 7). This is a fingerprint of a change of the mechanism acting at low and at high energies[23]. We note here that the same behaviour is shown also for QCT ics suggesting that the change of mechanism could be understood in term of classical mechanics. Moreover, we can observe a new change of the vibrational distributions at higher energies, around 2.5 eV (see insets in the panels). In fact around this energy, the integral cross sections of the lower vibrational products decrease, converging at energies higher than 4 eV to a common trend for the ics of all the final states. Until there, the population of the endothermic vibrational channels (from v'=4 onward) is practically negligible, although a considerable number of vibrational states (8) are energetically available.

In Fig. 8 product vibrationally resolved rates obtained in the ground state approximation are shown. The final state resolved rates obtained with the mixed QM-CC/QCT ics database are represented with solid curves; they can be used directly into applied models where a state resolved chemical network is implemented. At lower temperatures, where only the exothermic channels contribute, the relative importance of the rate coefficient for $v' = 0$ is lower, being the reaction rate for $v' = 2$ the largest until $\sim$ 1,000 K. All the vibrational channel rates show a maximum that moves towards lower temperatures with the increase of the vibrational quantum number, starting from $\sim$1,000 K for $v' = 3$ until $\sim$8,000 K for $v' = 0$. Quantum discrepancies can be more easily appreciated in this state resolved figure, compared to Fig. 5; in particular, we can see that they are relevant up to 1,000 K. In this range of temperatures, endothermic channels (from v'=4 onward) are negligible and have essentially a classical behaviour. The only small differences with QCT rates appear near

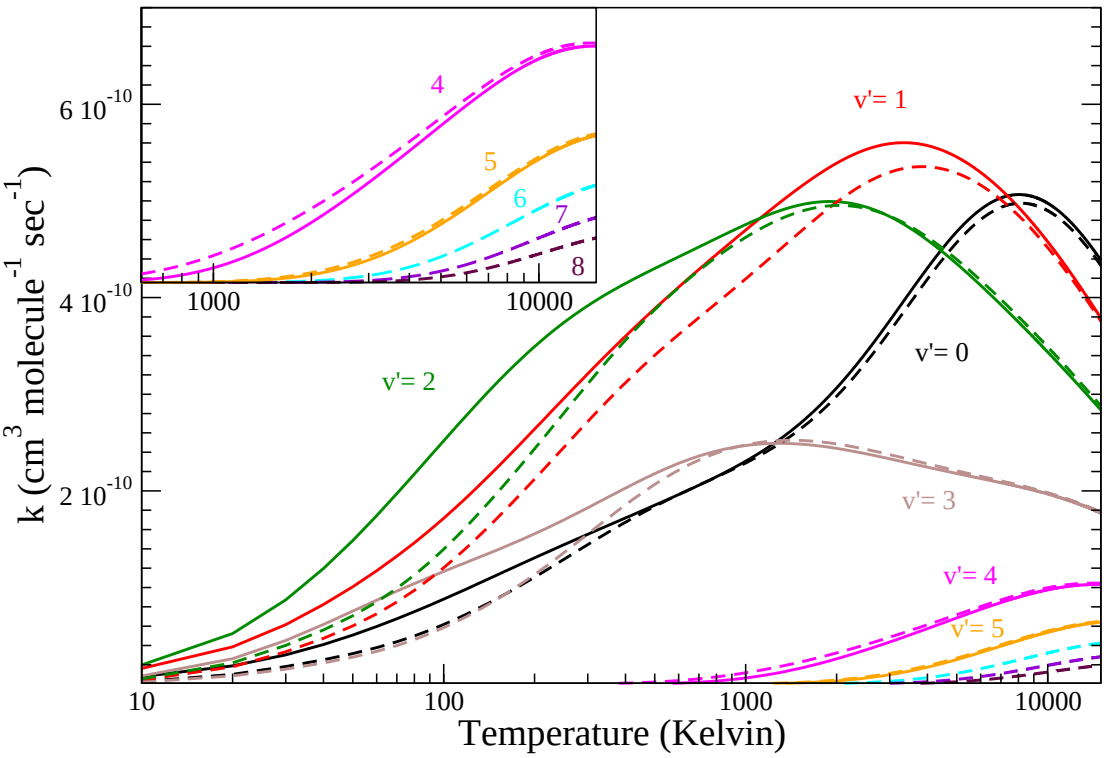

Figure 8 Esposito et al

Figure 8: Product vibrationally selected rate constants as a function of temperature in ground state approximation. Solid lines are obtained integrating a mixed QM-CC/QCT ics database (see text for details) while dashed lines are present QCT results. Black, red, green, blue, brown, magenta, orange, cyan, violet and indigo colours are for v' = 0,1,2,3,4,5,6,7,8 and 9, respectively.

the thresholds, where QCT results overestimate the yields probably because of the zero point energy and binning issues. From ∼8,000 K the rate coefficients decrease with the H_2^+ vibrational quantum number.

References

(1) Capitelli, M. et al. Non-equilibrium Plasma Kinetics: a State-to-State Approach. *Plasma Sources Sci. Technol.* **2007**, *16*, S30.

(2) Capitelli, M.; Celiberto, R.; Esposito, F.; Laricchiuta, A. Molecular Dynamics For State-to-State Kinetics of Non-equilibrium Molecular Plasmas: State of Art and Perspectives. *Plasma Process. Polym.* **2009**, *6*, 279.

(3) Cavallotti, C.; Leonori, F.; Balucani, N.; Nevrly, V.; Bergeat, A.; Falcinelli, S.; Vanuzzo, G.; Casavecchia, P. Relevance of the Channel Leading to Formaldehyde + Triplet Ethylidene in the O(3P) + Propene Reaction under Combustion Conditions. *J. Phys. Chem. Letters* **2014**, *5*, 4213.

(4) Capitelli, M.; Colonna, G.; Esposito, F. On the Coupling of Vibrational Relaxation with the Dissociation-Recombination Kinetics: from Dynamics to Aerospace Applications. *J. Phys. Chem. A* **2004**, *108*, 8930.

(5) Armenise, I.; Esposito, F. N2, O_2, NO State-to-State Vibrational Kinetics in Hypersonic Boundary Layers: the Problem of Rescaling Rate Coefficients to Uniform Vibrational Ladders. *Chem. Phys.* **2015**, *446*, 30.

(6) Panesi, M.; Jaffe, R. L.; Schwenke, D. W.; Magin, T. E. Rovibrational Internal Energy Transfer and Dissociation of $N_2^1\Sigma_g^+$ - $N^4\Sigma_u$ System in Hypersonic Flows. *J. Chem. Phys.* **2013**, *138*, 044312.

(7) Capitelli, M.; Celiberto, R.; Colonna, G.; D'Ammando, G.; De Pascale, O.; Diomede, P.; Esposito, F.; Gorse, C.; Laricchiuta, A.; Longo, S.; Pietanza, D.; Taccogna, F. Plasma Kinetics in Molecular Plasmas and Modeling of Reentry Plasmas. *Plasma Phys. Control. Fusion* **2011**, *53*, 124007.

(8) Coppola, C. M.; Longo, S.; Capitelli, M.; Palla, F.; Galli, D. Vibrational Level Population of H_2 and H_2^+ in the Early Universe. *Astrophys. J. Suppl. Ser.* **2011**, *193*, 7.

(9) Galli, D.; Palla, F. The Dawn of Chemistry. *Annu. Rev. Astron. Astrophys.* **2013**, *51*, 163.

(10) Yankovsky, V.; Manuilova, R.; Babaev, A.; Feofilov, A.; Kutepov, A. Model of Electronic-Vibrational Kinetics of the O_3 and O_2 Photolysis Products in the Middle Atmosphere: Applications to Water Vapour Retrievals from SABER/TIMED 6.3 μm Radiance Measurements. *Int. J. Remote Sens.* **2011**, *32*, 3065.

(11) Stewart, B. A.; Stephens, T. N.; Lawrence, B. A.; McBane, G. C. Rovibrational Energy Transfer in Ne-$Li_2(A^1\Sigma_u^+, v{=}0)$: Comparison of Experimental Data and Results from Classical and Quantum Calculations. *J. Phys. Chem. A* **2010**, *114*, 9875.

(12) Capitelli, M. *Nonequilibrium Vibrational Kinetics*; Topics in Current Physics; Springer-Verlag, 1986; Vol. 39.

(13) Dove, J. E.; Teitelbaum, H. The Vibrational Relaxation of H_2. I. Experimental Measurements of the Rate of Relaxation by H_2, He, Ne, Ar, and Kr. *Chem. Phys.* **1974**, *6*, 431.

(14) Armenise, I.; Esposito, F.; Capitelli, M. Dissociation-Recombination Models in Hypersonic Boundary Layer Flows. *Chem.Phys.* **2007**, *336*, 83.

(15) Capitelli, M.; Ferreira, C.; Gordiets, B.; Osipov, A. *Plasma Kinetics in Atmospheric Gases*; Atomic, Optical and Plasma Physics; Springer Berlin / Heidelberg, 2000.

(16) Kim, J. G.; Boyd, I. D. State-resolved Thermochemical Nonequilibrium Analysis of Hydrogen Mixture Flows. *Phys. Fluids* **2012**, *24*, 086102.

(17) Bender, J. D.; Valentini, P.; Nompelis, I.; Paukku, Y.; Varga, Z.; Truhlar, D. G.; Schwartzentruber, T.; Candler, G. V. An improved potential energy surface and multi-temperature quasiclassical trajectory calculations of N_2 + N_2 dissociation reactions. *J. Chem Phys* **2015**, *143*.

(18) Althorpe, S.; Clary, D. Quantum Scattering Calculations on Chemical Reactions. *Ann. Rev. Phys. Chem.* **2003**, *54*, 493.

(19) De Fazio, D.; Aquilanti, V.; Cavalli, S.; Aguilar, A.; Lucas, J. M. Exact Quantum Calculations of the Kinetic Isotope Effect: Cross Sections and Rate Constants for the F+HD Reaction and Role of Tunneling. *J. Chem. Phys.* **2006**, *125*, 133109.

(20) Jambrina, P. G.; Alvarino, J. M.; Gerlich, D.; Hankel, M.; Herrero, V. J.; Saez-Rabanos, V.; Aoiz, F. J. Dynamics of the $D^+ + H_2$ and $H^+ + D_2$ Reactions: a Detailed Comparison between Theory and Experiment. *Phys. Chem. Chem. Phys.* **2012**, *14*, 3346.

(21) Mielke, S.; Peterson, K.; Schwenke, D.; Garrett, B.; Truhlar, D.; Michael, J.; Su, M.-C.; Sutherland, J. H+H_2 Thermal Reaction: A Convergence of Theory and Experiment. *Phys. Rev. Lett.* **2003**, *91*.

(22) Aquilanti, V.; Cavalli, S.; Fazio, D. D.; Volpi, A.; Aguilar, A.; Lucas, J. M. Benchmark Rate Constants by the Hyperquantization Algorithm. The F + H_2 Reaction for Various Potential Energy Surfaces: Features of the Entrance Channel and of the Transition State, and Low Temperature Reactivity. *Chemical Physics* **2005**, *308*, 237, Reaction Dynamics in the Gas Phase.

(23) De Fazio, D. The H + $HeH^+ \rightarrow$ He + H_2^+ Reaction from the Ultra-Cold Regime to the Three-Body Breakup: Exact Quantum Mechanical Integral Cross Sections and Rate Constants. *Phys. Chem. Chem. Phys.* **2014**, *16*, 11662.

(24) Pack, R.; Walker, R.; Kendrick, B. Three-Body Collision Contributions to Recombination and Collision-Induced Dissociation. I. Cross Sections. *J. Chem. Phys.* **1998**, *109*, 6701.

(25) Perez-Rios, J.; Ragole, S.; Wang, J.; Greene, C. H. Comparison of Classical and Quantal Calculations of Helium Three-Body Recombination. *J. Chem. Phys.* **2014**, *140*, 044307.

(26) Kolakkandy, S.; Giri, K.; Sathyamurthy, N. Collision-Induced Dissociation in (He, H_2^+)(v = 0-2; j = 0-3)) System: a Time-Dependent Quantum Mechanical Investigation. *J. Chem. Phys.* **2012**, *136*, 244312.

(27) Bovino, S.; Schleicher, D. R. G.; Grassi, T. Primordial Star Formation: Relative Impact of H2 Three-Body Rates and Initial Conditions. *Astron. Astrophys.* **2013**, *561*, A13.

(28) Forrey, R. C. Sturmian Theory of Three-Body Recombination: Application to the Formation of H_2 in Primordial Gas. *Phys. Rev. A* **2013**, *88*, 052709.

(29) Esposito, F.; Capitelli, M. Selective Vibrational Pumping of Molecular Hydrogen Via Gas Phase Atomic Recombination. *J. Phys. Chem. A* **2009**, *113*, 15307.

(30) Kumar, S.; Sathyamurthy, N. Competition between Exchange and Dissociation Processes in He+H_2^+ Collisions. *Chem. Phys.* **1989**, *137*, 25.

(31) Azriel, V. M.; Kolesnikova, E. V.; Rusin, L. Y.; Sevryuk, M. B. Dynamical Mechanisms of Direct Three-Body Recombination. *J. Phys. Chem. A* **2011**, *115*, 7055.

(32) Miller, W. The Classical S-matrix: a More Detailed Study of Classically Forbidden Transitions in Inelastic Collissions. *Chem. Phys. Lett.* **1970**, *7*, 431.

(33) Marcus, R. A. Theory of Semiclassical Transition Probabilities (S Matrix) for Inelastic and Reactive Collisions. *J. Chem. Phys.* **1971**, *54*, 3965.

(34) Truhlar, D. G.; Garrett, B. C. Variational Transition State Theory. *Ann. Rev. Phys. Chem.* **1984**, *35*, 159.

(35) Miller, W. *Dynamics of Molecules and Chemical Reactions - Beyond Transition State Theory: Rigorous Quantum Approaches for Determining Chemical Reaction Rates*; John Zhang and Robert Wyatt, Eds., Marcel Dekker, Inc., 1995.

(36) Craig, I. R.; Manolopoulos, D. E. A Refined Ring Polymer Molecular Dynamics Theory of Chemical Reaction Rates. *J. Chem. Phys.* **2005**, *123*, 034102.

(37) McGuire, P.; Kouri, D. J. Quantum Mechanical Close Coupling Approach to Molecular Collisions. jz-Conserving Coupled States Approximation. *J. Chem. Phys.* **1974**, *60*, 2488.

(38) Khare, V.; Kouri, D. J.; Baer, M. Infinite Order Sudden Approximation for Reactive Scattering. I. Basic l-Labeled Formulation. *J. Chem. Phys.* **1979**, *71*, 1188.

(39) Huarte-Larranaga, F.; Gimenez, X.; Aguilar, A. The Application of Complex Absorbing Potentials to an Invariant Embedding Scattering Method: I. Theory and Computational Details. *J. Chem. Phys.* **1998**, *109*, 5761.

(40) De Fazio, D.; F. Castillo, J. State-to-State Three-Atom Reactive Scattering using Adiabatic Rotation Approximations. *Phys. Chem. Chem. Phys.* **1999**, *1*, 1165.

(41) Gonzalez-Lezana, T. Statistical Quantum Studies on Insertion Atom-Diatom Reactions. *Int. Rev. Phys. Chem.* **2007**, *26*, 29.

(42) Jambrina, P. G.; Alvarino, J. M.; Aoiz, F. J.; Herrero, V. J.; Saez-Rabanos, V. Reaction dynamics of the $D^+ + H_2$ system. A comparison of theoretical approaches. *Phys. Chem. Chem. Phys.* **2010**, *12*, 12591.

(43) Connor, J. N. L. Meldola Medal Lecture. Molecular Collisions and the Semiclassical Approximation. *Chem. Soc. Rev.* **1976**, *5*, 125.

(44) Miller, W. H. The Semiclassical Initial Value Representation: A Potentially Practical Way for Adding Quantum Effects to Classical Molecular Dynamics Simulations. *J. Phys. Chem. A* **2001**, *105*, 2942.

(45) C. Tully, J. Mixed Quantum-Classical Dynamics. *Faraday Discuss.* **1998**, *110*, 407.

(46) Wardlaw, D. M.; Marcus, R. A. *Advances in Chem. Phys.*; John Wiley & Sons, Inc., 2007; p 231.

(47) Bonnet, L. Classical Dynamics of Chemical Reactions in a Quantum Spirit. *Int. Rev. Phys. Chem.* **2013**, *32*, 171.

(48) Xiahou, C.; Connor, J. N. L.; Zhang, D. H. Rainbows and Glories in the Angular Scattering of the State-to-State F + H_2 Reaction at Etrans = 0.04088 eV. *Phys. Chem. Chem. Phys.* **2011**, *13*, 12981.

(49) Sokolovski, D.; De Fazio, D.; Cavalli, S.; Aquilanti, V. On the Origin of the Forward Peak and Backward Oscillations in the F + $H_2(v = 0) \rightarrow HF(v' = 2)$ + H Reaction. *Phys. Chem. Chem. Phys.* **2007**, *9*, 5664.

(50) Sokolovski, D.; Sen, S. K.; Aquilanti, V.; Cavalli, S.; De Fazio, D. Interacting Resonances in the F+H_2 Reaction Revisited: Complex Terms, Riemann Surfaces, and Angular Distributions. *J. Chem. Phys.* **2007**, *126*, 084305.

(51) Cavalli, S.; Aquilanti, V.; Mundim, K. C.; De Fazio, D. Theoretical Reaction Kinetics Astride the Transition between Moderate and Deep Tunneling Regimes: The F + HD Case. *J. Phys. Chem. A* **2014**, *118*, 6632.

(52) De Fazio, D.; Cavalli, S.; Aquilanti, V.; Buchachenko, A. A.; Tscherbul, T. V. On the Role of Scattering Resonances in the F + HD Reaction Dynamics. *J. Phys. Chem. A* **2007**, *111*, 12538.

(53) Bovino, S.; Tacconi, M.; Gianturco, F. A.; Galli, D. Ion Chemistry in the Early Universe: Revisiting the Role of HeH^+ With New Quantum Calculations. *Astron.Astrophys.* **2011**, *529*, A140.

(54) Gamallo, P.; Akpinar, S.; Defazio, P.; Petrongolo, C. Quantum Dynamics of the Reaction H(2S) + $HeH^+(X^1\Sigma^+) \rightarrow H_2^+(X^2\Sigma_g^+)$ + He(1S) from Cold to Hyperthermal Energies: Time-Dependent Wavepacket Study and Comparison with Time-Independent Calculations. *J. Phys. Chem. A* **2014**, *118*, 6451.

(55) Ramachandran, C.; De Fazio, D.; Cavalli, F., S.and Tarantelli; Aquilanti, V. Revisiting the Potential Energy Surface for the Reaction at the Full Configuration Interaction Level. *Chem. Phys. Lett.* **2009**, *469*, 26.

(56) Lepp, S.; Stancil, P. C.; Dalgarno, A. Atomic and Molecular Processes in the Early Universe. *J. Phys. B: At. Mol. Opt. Phys.* **2002**, *35*, R57.

(57) Hirata, C. M.; Padmanabhan, N. Cosmological Production of H_2 Before the Formation of the First Galaxies. *Mon. Not. Roy. Astron. Soc.* **2006**, *372*, 1175.

(58) Schleicher, D. R. G.; Galli, D.; Palla, F.; Camenzind, M.; Klessen, R. S.; Bartelmann, M.; Glover, S. C. O. Effects of Primordial Chemistry on the Cosmic Microwave Background. *Astron. Astrophys.* **2008**, *490*, 521.

(59) Sidis, V. Diabatic Excited States of the HeH_2^+ Molecular Ion for the Charge Exchange-Excitation Reaction: $He^+ + H_2 \rightarrow HeH^+ + H$. *Chem. Phys.* **1996**, *209*, 313.

(60) Palmieri, P.; Puzzarini, C.; Aquilanti, V.; Capecchi, G.; Cavalli, S.; De Fazio, D.; Aguilar, A.; Gimenez, X.; Lucas, J. M. Ab Initio Dynamics of the He + $H_2^+ \rightarrow HeH^+$ +H Reaction: a New Potential Energy Surface and Quantum Mechanical Cross-Sections. *Mol. Phys.* **2000**, *98*, 1835.

(61) Chu, T.-S.; Lu, R.-F.; Han, K.-L.; Tang, X.-N.; Xu, H.-F.; Ng, C. Y. A Time-Dependent Wave-Packet Quantum Scattering Study of the Reaction H_2^+(v=0-2,4,6; j=1)+He $\rightarrow$ HeH^++H. *J. Chem. Phys.* **2005**, *122*, 244322.

(62) De Fazio, D.; de Castro-Vitores, M.; Aguado, A.; Aquilanti, V.; Cavalli, S. The He + H_2^+ $\rightarrow$ HeH^+ + H Reaction: Ab Initio Studies of the Potential Energy Surface, Benchmark Time-Independent Quantum Dynamics in an Extended Energy Range and Comparison with Experiments. *J. Chem. Phys.* **2012**, *137*, 244306.

(63) Harris, G. J.; Lynas-Gray, A. E.; Miller, S.; Tennyson, J. The Role of HeH^+ in Cool Helium-rich White Dwarfs. *Astrophys. J. Lett.* **2004**, *617*, L143.

(64) Roberge, W.; Dalgarno, A. The Formation and Destruction of HeH^+ in Astrophysical Plasmas. *Astrophys. J.* **1982**, *255*, 489.

(65) Galli, D.; Palla, F. The Chemistry of the Early Universe. *Astron. Astrophys.* **1998**, *335*, 403.

(66) Defazio, P.; Gamallo, P.; Petrongolo, C. Nonadiabatic Dynamics of O(^{1}D) + $N_2(X^1\Sigma_g^+)$$\rightarrow$ O(^{3}P)+$N_2(X^1\Sigma_g^1)$ on Three Coupled Potential Surfaces: Symmetry, Coriolis, Spin-Orbit, and Renner-Teller Effects. *J. Chem. Phys.* **2012**, *136*.

(67) Karpas, Z.; Anicich, V.; Huntress, W. T. An Ion Cyclotron Resonance Study of Reactions of Ions with Hydrogen Atoms). *J. Chem. Phys.* **1979**, *70*, 2877.

(68) Rutherford, J. A.; Vroom, D. A. Study of the Reactions H_2^+ + He$\rightarrow$$HeH^+$+H and HeH^+ + H$\rightarrow$$H_2^+$+He Using Crossed Beam Techniques. *J. Chem. Phys.* **1973**, *58*, 4076.

(69) De Fazio, D.; Gianturco, F. A.; Rodriguez-Ruiz, J. A.; Tang, K. T.; Toennies, J. P. A Semiclassical Model for Polarization Forces in Collisions of Electrons and Positrons with Helium Atoms. *J. Phys. B: At. Mol. Opt. Phys.* **1994**, *27*, 303.

(70) Velilla, L.; Lepetit, B.; Aguado, A.; Beswick, J. A.; Paniagua, M. The H_3^+ Rovibrational Spectrum Revisited with a Global Electronic Potential Energy Surface. *J. Chem. Phys.* **2008**, *129*, 084307.

(71) Gao, B. Quantum Langevin Model for Exoergic Ion-Molecule Reactions and Inelastic Processes. *Phys. Rev. A* **2011**, *83*, 062712.

(72) Pattengill, M. *Atom-Molecule Collision Theory*; Springer, 1979.

(73) Porter, R.; Raff, L. In *Dynamics of Molecular Collisions*; Miller, W., Ed.; Modern Theoretical Chemistry; Springer US, 1976; Vol. 2.

(74) Esposito, F. Dinamica Quasiclassica di Processi Collisionali Inelastici e Reattivi in Sistemi H + H_2 e N + N_2 Rotovibrazionalmente Risolti. PhD Thesis, Università degli Studi di Bari, Bari, 1999.

(75) Esposito, F.; Capitelli, M. QCT Calculations for the Process $N_2(v)$+N $\rightarrow N_2(v')$+N in the Whole Vibrational Range. *Chem.Phys.Lett.* **2006**, *418*, 581.

(76) Esposito, F.; Capitelli, M. The Relaxation of Vibrationally Excited O_2 Molecules by Atomic Oxygen. *Chem.Phys.Lett.* **2007**, *443*, 222.

(77) Akpinar, S.; Armenise, I.; Defazio, P.; Esposito, F.; Gamallo, P.; Petrongolo, C.; Sayos, R. Quantum Mechanical and Quasiclassical Born-Oppenheimer Dynamics of the Reaction $N_2(X^1\Sigma_g^+)$+$O(^3P)\rightarrow N(^4S)$+$NO(X^2\Pi)$. *Chem. Phys.* **2012**, *398*, 81.

(78) Esposito, F.; Capitelli, M. Quasiclassical Trajectory Calculations of Vibrationally Specific Dissociation Cross-Sections and Rate Constants for the Reaction O+O_2(v) $\rightarrow$ 3O. *Chem.Phys.Lett.* **2002**, *364*, 180.

(79) Blais, N. C.; Truhlar, D. G. Monte Carlo Trajectory Study of Ar+H_2 Collisions. I. Potential Energy Surface and Cross Sections for Dissociation, Recombination, and Inelastic Scattering. *J. Chem. Phys.* **1976**, *65*, 5335.

(80) *See Supplementary Material No. for a comparison between the energy levels (including the quasi-bound states) of HeH^+ calculated with QM and WKB methods. For information on Supplementary Material, see*

(81) Bonnet, L.; Rayez, J.-C. Gaussian Weighting in the Quasiclassical Trajectory Method. *Chem. Phys. Lett.* **2004**, *397*, 106.

(82) Homayoon, Z.; Jambrina, P. G.; Aoiz, F. J.; Bowman, J. M. Communication: Rate coefficients from Quasiclassical Trajectory Calculations from the Reverse Reaction: the Mu+H_2 Reaction Re-visited. *J. Chem. Phys.* **2012**, *137*, 021102.

(83) De Fazio, D.; Lucas, J. M.; Aquilanti, V.; Cavalli, S. Exploring the Accuracy Level of New Potential Energy Surfaces for the F + HD Reactions: from Exact Quantum Rate Constants to the State-to-State Reaction Dynamics. *Phys. Chem. Chem. Phys.* **2011**, *13*, 8571.

(84) Skouteris, D.; Castillo, J.; Manolopoulos, D. ABC: a Quantum Reactive Scattering Program. *Comp. Phys. Comm.* **2000**, *133*, 128.

(85) Colavecchia, F. D.; Mrugala, F.; Parker, G. A.; Pack, T. R. Accurate Quantum Calculations on Three-Body Collisions in Recombination and Collision-Induced Dissociation. II. The Smooth Variable Discretization Enhanced Renormalized Numerov Propagator. *J. Chem. Phys.* **2003**, *118*, 10387.

(86) Manolopoulos, D. E. An Improved Log Derivative Method for Inelastic Scattering. *J. Chem. Phys.* **1986**, *85*, 6425.

(87) Chao, S. D.; Harich, S. A.; Xu Dai, D.; Wang, C. C.; Yang, X.; Skodje, R. T. A Fully State- and Angle-Resolved Study of the H+HD→D+H_2 Reaction: Comparison of a Molecular Beam Experiment to Ab Initio Quantum Reaction Dynamics. *J. Chem. Phys.* **2002**, *117*, 8341.

(88) Gioumousis, G.; Stevenson, D. P. Reactions of Gaseous Molecule Ions with Gaseous Molecules. V. Theory. *J. Chem. Phys.* **1958**, *29*, 294.

(89) Leforestier, C. Competition between Dissociation and Exchange Processes in a Collinear A + BC Collision: Comparison of Quantum and Classical Results. *Chem. Phys. Lett.* **1986**, *125*, 373.

(90) Nobusada, K.; Sakimoto, K. A Quantum Mechanical Study of He+H_2 →He+H+H in the Energy Range 5-10 eV. *Chem. Phys. Lett.* **1998**, *288*, 311.

(91) Sakimoto, K. A Semiclassical Study of Dissociation Dynamics in He+H_2 Collisions. *Chem.Phys.* **1998**, *236*, 123.

(92) Sokolovski, D.; Akhmatskaya, E.; Echeverria-Arrondo, C.; De Fazio, D. Complex Angular Momentum Theory of State-to-State Integral Cross Sections: Resonance Effects in the F + HD → HF($v\prime$= 3) + D Reaction. *Phys. Chem. Chem. Phys.* **2015**, *17*, 18577.

(93) Bovino, S.; Gianturco, F.; Tacconi, M. Chemical Destruction of Rotationally "hot" HeH_+: Quantum Cross Sections and Mechanisms of its Reaction with H. *Chem. Phys. Lett.* **2012**, *554*, 47.

(94) Gamallo, P.; Defazio, P.; Gonzalez, M.; Paniagua, M.; Petrongolo, C. Born-Oppenheimer and Renner-Teller Coupled-Channel Quantum Reaction Dynamics of O(^{3}P) + H_2^+($X^2\Sigma_g^+$) Collisions. *Phys. Chem. Chem. Phys.* **2015**, *17*, 23392.

(95) Aquilanti, V.; Mundim, K.; Cavalli, S.; De Fazio, D.; Aguilar, A.; Lucas, J. Exact Activation Energies and Phenomenological Description of Quantum Tunneling For Model Potential Energy Surfaces. The Reaction at Low Temperature. *Chem. Phys.* **2012**, *398*, 186.

(96) Aguado, A.; Suarez, C.; Paniagua, M. Accurate Fit of the Two Lowest Excited-State Potential-Energy Surfaces for Doublet HeH_2^+. *J. Chem. Phys.* **1993**, *98*, 308.

(97) Gordillo-Vazquez, F. J.; Kunc, J. A. Statistical-Mechanical Calculations of Thermal Properties of Diatomic Gases. *J. Appl. Phys.* **1998**, *84*, 4693.

(98) Esposito, F.; Gorse, C.; Capitelli, M. Quasi-Classical Dynamics Calculations and State-Selected Rate Coefficients for $H+H_2(v,j)\rightarrow 3H$ Processes: Application to the Global Dissociation Rate under Thermal Conditions. *Chem. Phys. Lett.* **1999**, *303*, 636.

(99) Bruno, D.; Capitelli, M.; Longo, S. DSMC Modelling of Vibrational and Chemical Kinetics for a Reacting Gas Mixture. *Chem. Phys. Lett.* **1998**, *289*, 141.

(100) Yano, R.; Suzuki, K.; Kuroda, H. Formulation and Numerical Analysis of Diatomic Molecular Dissociation using Boltzmann Kinetic Equation. *Phys. Fluids* **2007**, *19*, 017103.

(101) Coppola, C. M.; D'Introno, R.; Galli, D.; Tennyson, J.; Longo, S. Non-equilibrium H_2 Formation in the Early Universe: Energy Exchanges, Rate Coefficients, and Spectral Distortions. *Astrophys. J. Suppl. Ser.* **2012**, *199*, 16.

(102) Levine, R. D. *Molecular Reaction Dynamics*; Cambridge University Press, 2005.

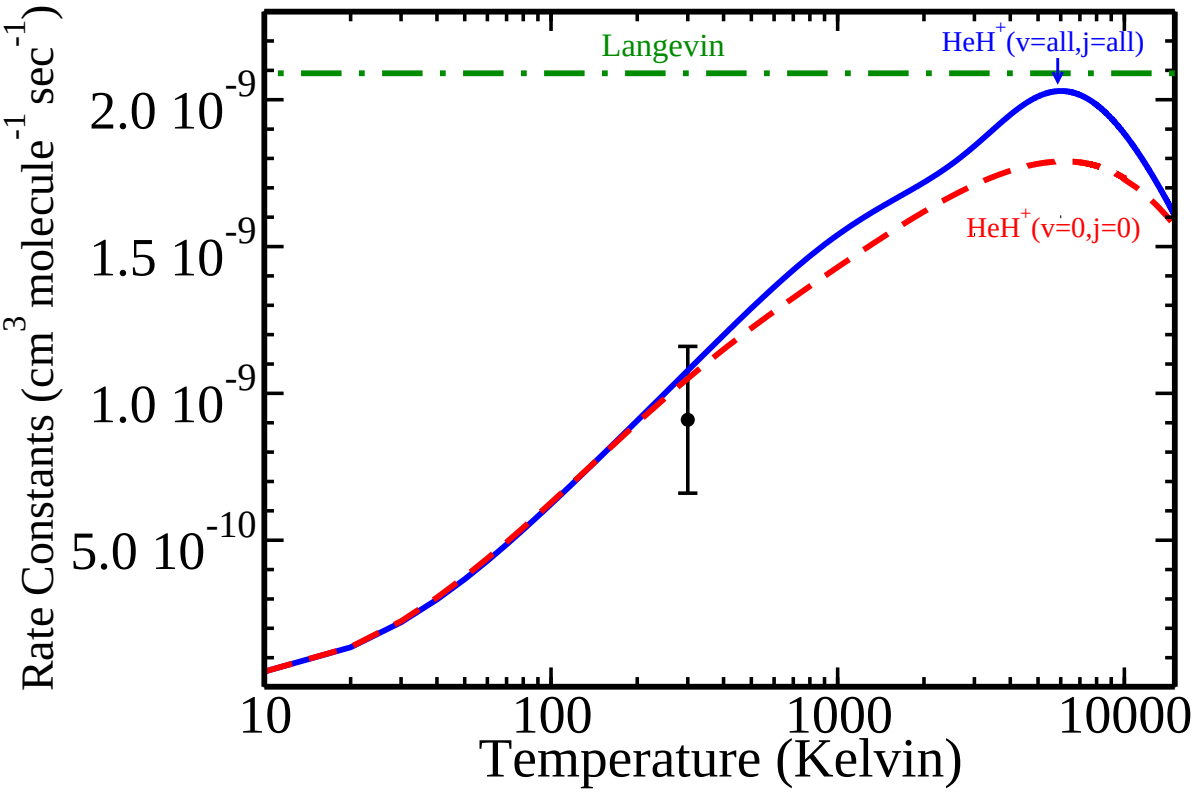

TOC Esposito et al